Chemistry, Physics and Technology of Surface. 2025. V. 16. N 4. P. 508-520

PACS 82.33.Ln; 82.70.Gg; 36.20.-r doi: 10.15407/hftp16.04.508

D.K. Honcharuk [1], A.P. Maletsky [2], T.P. Poltoratska [1], L.O. Kernosenko [1], N.O. Pasmurtceva [1], M.M. Lazarenko [3], S.M. Dybkova [1], L.S. Rieznichenko [1], T.G. Gruzina [1], V.I. Podolska [1], Yu.M. Samchenko [1]

INCORPORATION OF GOLD NANOPARTICLES BY *IN SITU* AND *EX SITU* METHODS INTO HYBRID HYDROGELS FOR MEDICAL PURPOSES

[1] F.D. Ovcharenko Institute of Biocolloid Chemistry of National Academy of Sciences of Ukraine
42 Academician Vernadsky Blvd., Kyiv, 03142, Ukraine, E-mail: goncarukdima325@gmail.com
[2] Filatov Institute of eye diseases and tissue therapy of National Academy of Medical Sciences of Ukraine
49/51 Francuzsky Blvd., Odessa, 65061, Ukraine
[3] Taras Shevchenko National University of Kyiv
4 Academician Glushkov Ave., Kyiv, 03680, Ukraine

Polymer hydrogels occupy a special place among the materials currently used for implant manufacturing due to their structural similarity to the macromolecular components found in the human body. However, traditional hydrogels often have insufficient mechanical strength, biocompatibility and biological activity. To overcome these limitations, we have developed methods for synthesising composite hybrid hydrogels based on porous polyvinylformal and gold nanoparticles. The physical and chemical properties of these hydrogels have been shown to depend on the synthesis strategy employed for the composite material, as well as on the type and synthesis method of the nanoparticles that it contains.

The morphology of the synthesized hybrid hydrogels (based on Polyvinylformal and gold nanoparticles, incorporated by in situ and ex situ methods) was investigated by means of electron microscopy (SEM), while their chemical structure was confirmed by Fourier Transform Infrared Spectroscopy (FTIR). The elemental composition of the synthesised polymer nanocomposites was investigated using energy-dispersive X-ray spectroscopy (EDX), while their thermostability and thermolysis processes were analysed using thermogravimetric analysis (TG, TGA and DTG studies). The swelling kinetics of hybrid gels with incorporated gold nanoparticles in water, the rate of diffusion of incorporated anticancer preparation DOXrubicin and bactericide Albucide, as well as their acute toxicity using in vitro experiments, were studied.

The synthesised composite hybrid hydrogels, which are based on porous polyvinyl formal and gold nanoparticles, show great promise as implants for reconstructive surgery in the oculo-orbital region. They can also be used to fill postoperative cavities after tumour resection, ensuring sterility of the surgical field and preventing tumour recurrence.

***Keywords**: hydrogels, polyvinylformal, sponge, implants, gold nanoparticles, reconstructive surgery, orbital injuries*

INTRODUCTION

In recent decades, there has been an overall increase in craniofacial injuries, primarily due to man-made and criminal injuries to the eye and its orbit. The majority of orbital injuries involve disruption to the bone walls. Additionally, the number of patients affected by fighting in Ukraine has increased significantly. Combat mine-blast injuries are characterised by significant tissue damage to the eye and eye socket, and multiple shrapnel wounds, often in combination with facial and other injuries [1]. The most common facial fractures were of the orbital (26.3 %) and maxilla/zygoma (25.1 %), according to the findings of the Joint Facial and Invasive Neck Trauma (J-FAINT) Project (Iraq and Afghanistan: 2011–2016) [2]. Due to the increasing occurrence of ocular trauma, there is a growing demand for reconstructive surgery in the oculo-orbital region. Significant tissue loss and high infection rates are often the result of these injuries. Special strategies are required for wound care and tissue reconstruction [3, 4]. When performing such operations, ophthalmic surgeons need to use implant materials to replace soft tissue or bone. Currently, biological tissues such as autotissue (homo- and autografts, autologous fat and the broad fascia of the thigh) and allotissue are used as graft materials in orbital surgery. It should be noted that legal requirements and restrictions on the collection of donor material are

becoming more stringent in Ukraine and around the world each year. This makes it urgent to find a synthetic material that meets the necessary requirements for reconstructive surgery on the orbit and other parts of the facial skeleton, as well as for filling postoperative cavities.

Non-biological implants with a porous, three-dimensional structure that can integrate with surrounding tissues offer fundamentally new opportunities. In our opinion, a porous hydrogel based on polyvinylformal is a promising candidate for this application. Previous studies have demonstrated the high antimicrobial activity of such hydrogels [5] and their suitability for the immobilisation and prolonged release of a wide range of drugs [6, 7]. Due to their structural similarity to the macromolecular components found in the human body, polymer hydrogels occupy a special place among the materials currently used for implant manufacturing [8]. However, traditional hydrogels often have insufficient mechanical strength and biocompatibility, and lack biological activity – particularly the ability to stimulate the adhesion and growth of eukaryotic cells – which limits their use as implant materials [9]. To overcome these limitations, research in tissue engineering and regenerative medicine has focused on creating composite hybrid hydrogels incorporating metal nanoparticles. These composite hydrogels exhibit enhanced mechanical, physical, chemical and biological properties, which depend on the synthesis strategy of the composite material and the type and synthesis method of the nanoparticles in its composition. Among the various types of metal nanoparticles promising for use in composite hydrogels for medical purposes, gold nanoparticles (AuNPs) occupy a special place due to their unique physical and biological properties. For instance, AuNPs are widely used in cancer treatment approaches, such as photothermal and photodynamic therapy, and as an antiangiogenic agent and a vector for targeted delivery of anticancer drugs [10, 11]. The anti-inflammatory and antioxidant properties of AuNPs [12], as well as their capability to stimulate tissue regeneration, including bone [13], are equally important. The capability of AuNPs to stimulate cell adhesion to the hydrogel surface is also highly significant [14]. These biological properties determine the widespread use of AuNPs in creating nanocomposite hybrid hydrogels with specified characteristics [15–18]. Among the undeniable advantages of adding gold nanoparticles to composite hybrid hydrogel compositions, the biocompatibility and low irritancy of the resulting materials are especially notable [19].

Besides plastic surgery in the oculo-orbital area ehe synthesized hybrid material is intended to fill postoperative cavities after tumor resection and should ensure sterility of the surgical field and prevention of tumor recurrence.

This work focuses on developing methods for synthesising hybrid hydrogel materials containing gold nanoparticles bactericides and cytostatics with complex antitumour, disinfecting and regenerative action for reconstructive surgery in the oculo-orbital region and filling of postoperative cavities, as well as comparing two methods of incorporating gold nanoparticles into hydrogels (*in situ* and *ex situ*).

MATERIALS AND METHODS

Chloroauric acid ($HAuCl_4 \times 3H_2O$, ≥ 99.9 % trace metals basis, Sigma-Aldrich), DOXrubicin (DOX, 2 mg mL^{-1}, Ebeve), formaldehyde (37 %, LAB-SCAN), poly(vinyl alcohol) [PVA, 72 kDa linear, 98 %, AppliChem GmbH], sulfacetamide sodium (30 % solution, JSC Farmak), sulfuric acid, Triton X-100 (AppliChem GmbH) were used as received. Bidistilled water was used as the solvent in all experiments.

Synthesis of gold nanoparticles. Spherical gold nanoparticles (AuNPs) with an average diameter of 30 nm were synthesized at a gold concentration of 38.6 μg mL^{-1} via the hydrothermal method [20].

Infrared (IR) analysis was performed using a Fourier-transform infrared spectrometer (Shimadzu IRAffinity-1S) with an attenuated total reflection detector (Specac Quest ATR) from 4000 to 400 cm^{-1}, with an accumulation of 25–40 scans and a resolution of 4 cm^{-1}.

Synthesis of unfilled PVF-based sponges. Poly(vinyl alcohol) (PVA) was acetalized by condensation with formaldehyde in the presence of a sulfuric acid, as described previously [21].

In situ and ex situ methods for the incorporation of AuNPs into a PVF-based hydrogel matrix.

In situ method. The synthesis of AuNPs was carried out in the pore space of the hydrogel matrix. 7.65 g of PVA was swollen in 59.3 g of water for 1 h 25 min, after which 1.84 ml of 0.1 % $HAuCl_4$ solution was added, stirred for 5 min,

heated to 82 °C with stirring, cooled to 49 °C, 2.04 ml of 10 % Triton X100 solution was added, then 9.66 ml of 50 % sulfuric acid solution and 8.05 ml of formalin, after which the gel-forming composition was poured into molds, placed in a thermostat at 60 °C for 1 h, and left overnight at 40 °C.

Ex situ method. To incorporate the gold nanoparticles, the calculated amount of the suspension of pre-synthesized AuNPs was added under integrative stirring to the gel-forming composition (CAu final = 12.06 μg/ml by metal). After about 4 hours, the hydrogels were removed from the molds and intensively washed with distilled water to remove unreacted residues.

The morphology and structure of the PVF matrices were studied using a scanning electron microscope (Tescan Mira LMU) equipped with an energy-dispersive spectrometer (Oxford X-Max 80) and a sample preparation system (PECS Gatan 682).

The Fourier-transform infrared spectrometer (Shimadzu IRAffinity-1S) with an attenuated total reflection detector (Specac Quest ATR) was used to perform infrared (IR) analysis. The spectrum was scanned from 4000 to 400 cm^{-1}, with an accumulation of 25–40 scans and a resolution of 4 cm^{-1}. LabSolutions IR software (ver. 2.26) and OriginPro (ver.10.0.5.157) were used to process and visualize the data, respectively.

Doxorubicin (DOX) and Albucid (ALB) diffusion. For DOX incorporation, nano-composite hydrogels (~0.05 g) were equilibrated in 5 mL of DOX solution at a concentration of 0.235 mg mL^{-1} at 11 °C for 24 h. After DOX absorption, the samples were transferred into empty beakers to perform DOX release studies, and 10 mL of water were added. The samples were separated from the solutions by centrifugation and transferred to 10 mL of fresh water at the specified times. The concentration of DOX in the solution was quantified spectrophotometrically at 480 nm using a UV spectrometer Specord M40 (Carl Zeiss Industrielle Messtechnik GmbH, Germany). Diffusion of albucid was studied in a similar way (initial concentration – 0.025 mg mL^{-1}; maximum absorption – 260 nm). Hydrogel composites were impregnated by DOX and ALB solutions as well as by their mixture followed by study of their sorption and diffusion parameters.

Thermogravimetric analysis (TGA) measurements were performed using a Q1000 derivatograph (MOM, Hungary) in the range of 20–700 °C at a rate of 10 °/min. The weight loss of the samples during the measurement was determined using a VIBRA HT balances (Japan).

Swelling of hybrid hydrogels based on PVF and AuNPs. The swelling kinetics of PVF-based matrices was studied in water at room temperature (24 ± 1 °C). The samples reached an equilibrium degree of swelling within 10 minutes after contact with water, which is explained by the presence of an widespread network of open interconnected transport pores in the matrices.

The equilibrium degree of swelling of hydrogels in distilled water, (Q), was calculated using the formula:

$$Q = \frac{m_s - m_d}{m_d},$$

where m_s is the mass of the swollen hydrogel in the equilibrium state after 24 hours of swelling, and m_d is the mass of the completely dried xerogel after water evaporation. The hydrogel samples were incubated in a TS-1/80 SPN thermostat and weighed with an accuracy of 10^{-4} g on an AXIS analytical balance (Poland). Data are presented as mean standard deviation of three to five independent experiments. ANOVA was used for statistical data processing, $p < 0.05$ was considered reliable.

Enzymatic activity: Mg^{2+}-ATPase activity was determined according to the Methodological recommendations [22]. The AuNP–albucid conjugate, known for its pronounced cytotoxic effect, was used as a positive control [23].

Cytotoxicity: Conditioned media were obtained by incubating hydrogel samples in culture medium for 24 h. Cytotoxic effects were assessed using the MTT assay (cell metabolic activity) and crystal violet staining (number of adherent cells).

Genotoxicity: Genotoxic potential was analysed by the Comet assay (single-cell gel electrophoresis) on L929 cells, following the procedure described in [22].

RESULTS AND DISCUSSION

The results of FTIR spectroscopy, which was used to identify hydrophilic groups in the PVF matrices, are shown in Fig. 1. The peaks in Fig. 1 are predominantly associated with pure PVF [24].

Nevertheless, some distinctive PVA peaks were also detected at 3380, 2800–3000, 1664–1666, 1476, 1434, and 1242 cm^{-1}. The preservation of certain structural features, including the hydroxyl groups of the PVA precursor, is indicated by these peaks, and this preservation is found in the PVF matrices. The stretching vibration of the O-H groups, as evidenced by the widening of the peaks at 3354–3380 cm^{-1}, was attributed to intramolecular interactions and vibrational oscillations of adsorbed atmospheric water. The 1006 cm^{-1} band was found to be linked to the CO stretching vibration in the six-membered ring (see Fig. 1), along with the nearby C-C stretching vibration. PVA does not contain this band. Vibrational oscillations centred at 1006, 1066, 1132, and 1172 cm^{-1} were exhibited by the spectra of all PVF matrices. These oscillations [25] are specific to the cyclic sequence of bonds in the polymer structure. Two peaks, at 1096 and 1240 cm^{-1}, were observed in the PVA and PVF matrices and were assigned to hydroxyl groups. The vibrations of methylene groups' sp^3-hybridized carbon hydrogen bonds (CH_2) were observed at 2800–3000, 1300–1400, and below 700 cm^{-1} [26]. The intensity of the absorption bands related to skeleton vibrations was low and they were observed at 700–1100 cm^{-1} (stretching vibrations) and below 500 cm^{-1} (deformational vibrations) [26]. Notably, the FTIR spectra of the PVF-based nanocomposites did not reveal any identifiable presence of AuNPs.

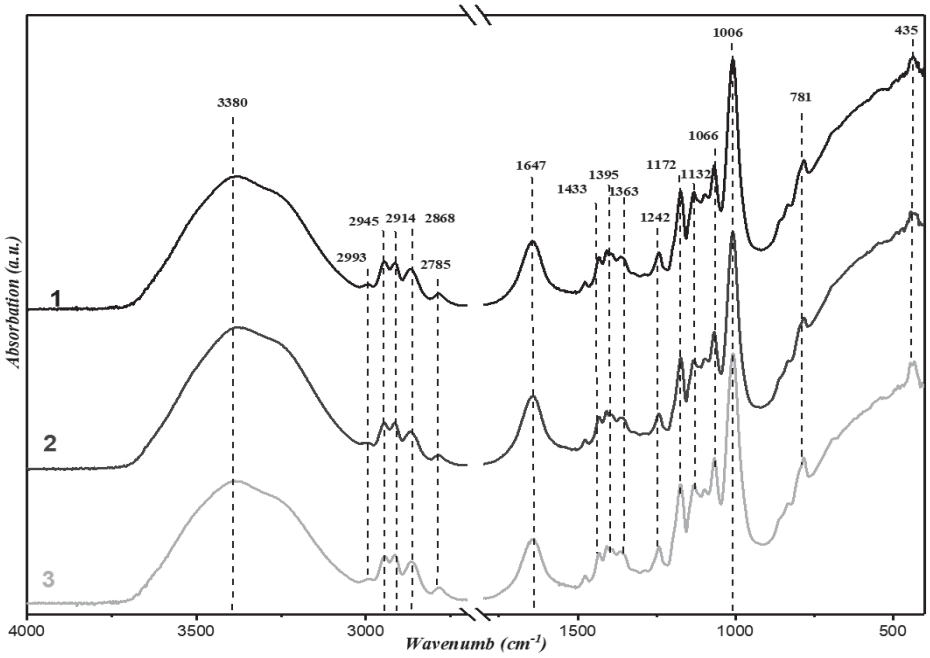

Fig. 1. FTIR spectrum of hybrid hydrogels: *1* – PVF; *2* – PVF + Au 12.06 μg/g; *3* – PVF + Au 24.12 μg/g

SEM analysis. Fig. 2 shows the appearance of hybrid sponge hydrogels based on PVF, with AuNPs incorporated by *in situ* and *ex situ* methods. With increasing magnification, it is evident that the surface of the gels is covered with numerous macropores, each with a diameter of about 50–100 μm. There are also numerous small pores, measuring about 3–7 μm, which appear predominantly sealed, in contrast to the open transport macropores. Notably, in gels containing gold nanoparticles incorporated in situ, the transport pores are uniformly distributed and sized over a smooth surface. In contrast, the surface of gels obtained by the ex situ method is much more wrinkled, with less uniform transport pore distribution.

A more detailed SEM analysis of the PVF surface morphology with incorporated gold nanoparticles is shown in Fig. 3. The images at higher magnifications confirm the presence of both large transport pores and smaller sealed pores.

Fig. 4 shows the pores present on the surface of the gels in more detail. The pore size and pore wall thickness are approximately the same in both gels under study (50–100 μm and about 3–10 μm, respectively).

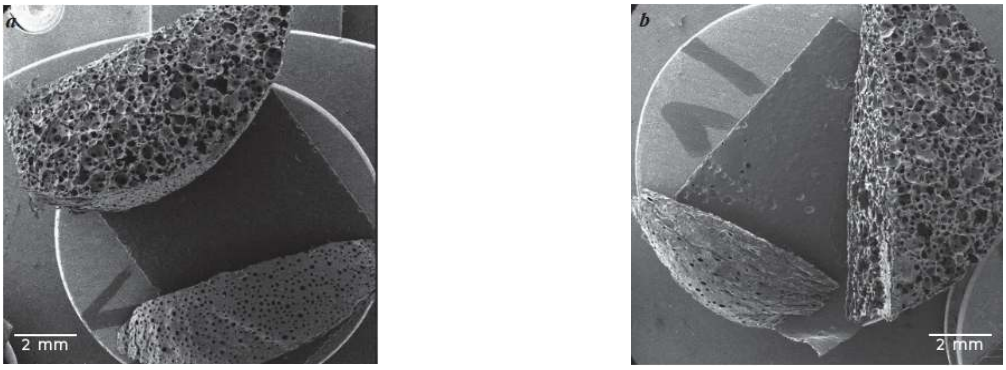

Fig. 2. Appearance of PVF with AuNPs incorporated by *in situ* (*a*) and *ex situ* (*b*) methods

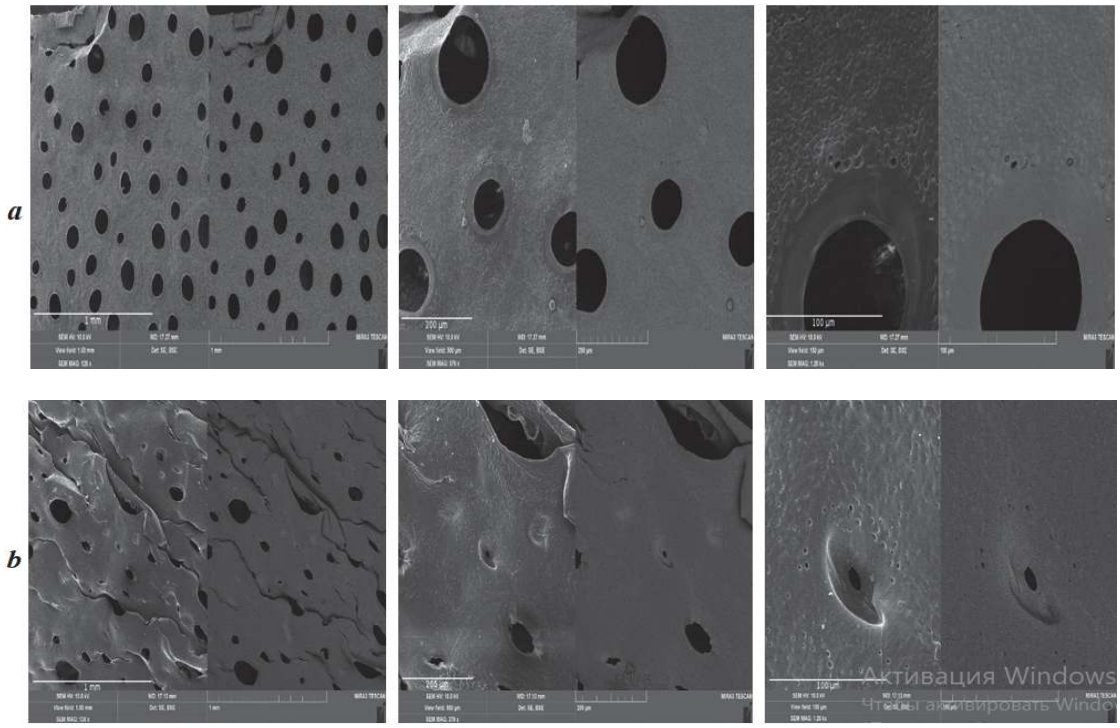

Fig. 3. PVF surface with gold nanoparticles, which are incorporated by *in situ* (*a*) and *ex situ* methods (*b*) (zoom 126 x; 379 x; 1.26 кх)

Additionally, SEM micrographs of the fracture surfaces (Fig. 5) reveal the porous sponge-like internal architecture of both *in situ* and *ex situ* hydrogels, with pore walls of ~0.5–1 μm.

The morphology of the fracture surfaces of hybride hydrogels is illustrated in Fig. 5. The internal structure of both *in situ* and *ex situ* gels can be described as a sponge with numerous pores (dark areas) between the polysaccharide matrices. These pores create because of water evaporating between the cross-linked polymer matrices during freeze-drying. A fairly similar pattern is observed in both cases, but it should be noted that the pore size is slightly larger in the case of *in situ* synthesis than in the case of *ex situ* synthesis. Generally, deep pores form a fairly symmetrical, honeycomb-like structure with a pore size of around 1.5–2.5 μm and a wall thickness of around 0.5–1 μm.

The EDX spectra (Fig. 6) confirm that all studied samples contain C, O, Au as primary elements. The concentration of gold nanoparticles was about twice as high when incorporated by the *ex situ* method than by the *in situ* method, but the latter provided much higher uniformity of gold distribution.

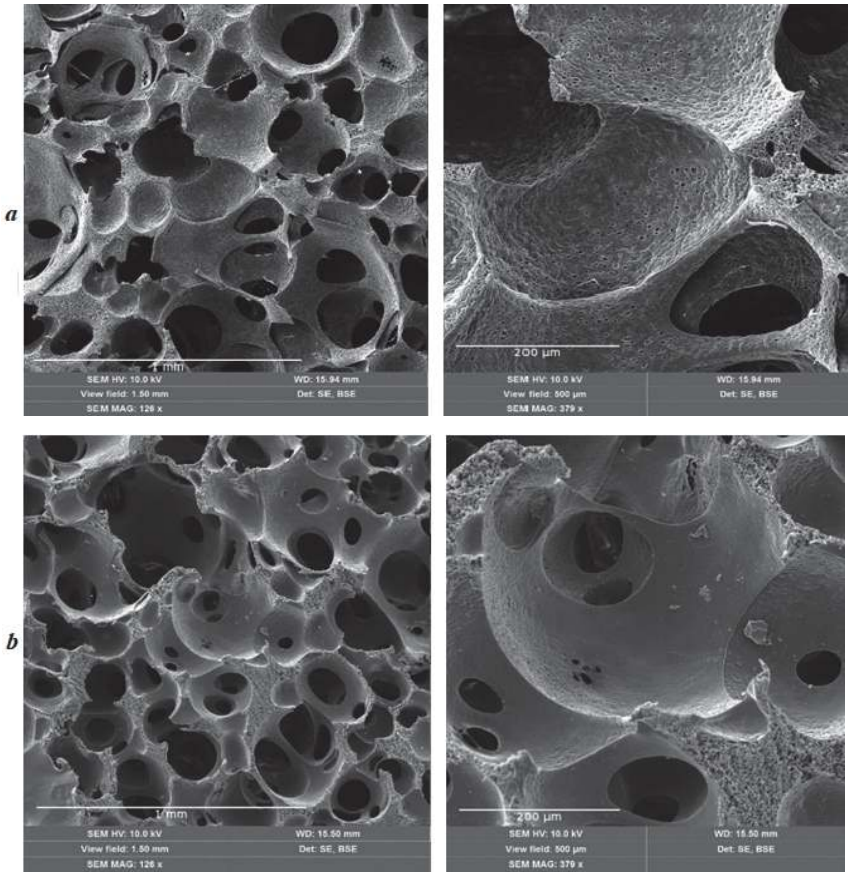

Fig. 4. Pores on the PVF surface with gold nanoparticles incorporated by *in situ* (*a*) and *ex situ* (*b*) methods (zoom 126 x; 379 x)

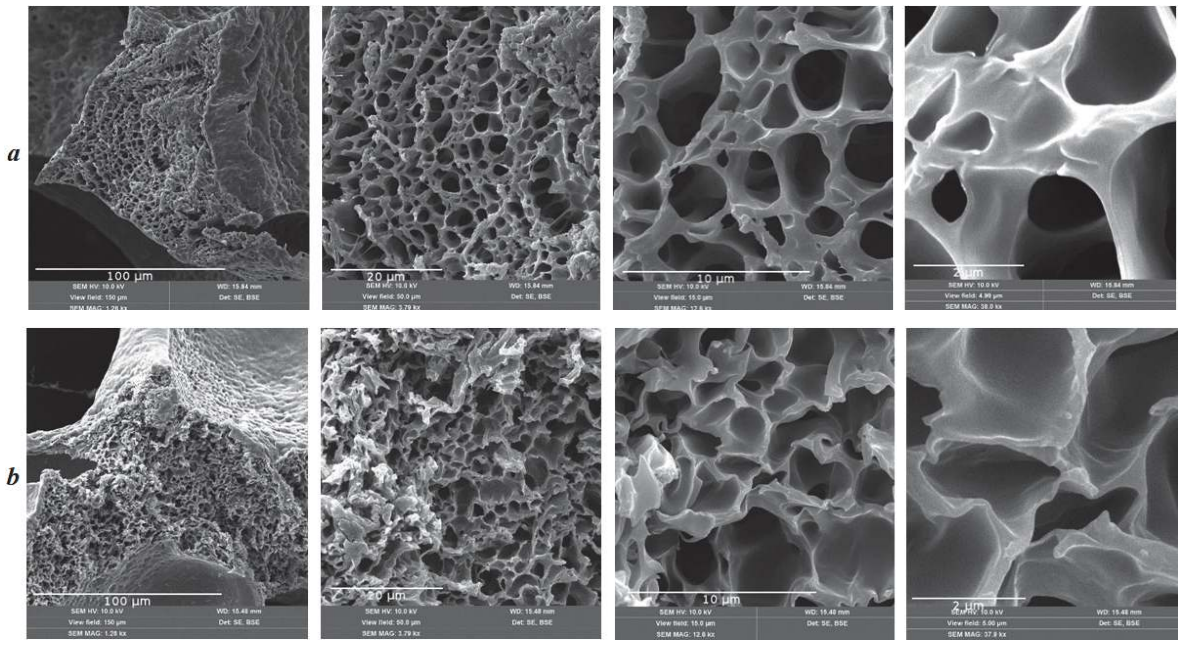

Fig. 5. Fracture of PVF with gold nanoparticles incorporated by *in situ* (*a*) and *ex situ* (*b*) methods (zoom 126 x; 379 x) methods (zoom 1.26 kx; 3.79 kx; 12.6 kx; 38.0 kx)

Swelling. The samples reached an equilibrium degree of swelling within 10 minutes after contact with water, which is explained by the presence of a widespread network of open interconnected transport pores in the matrices. To compare the two methods of incorporation of AuNPs into PVF sponges, their swelling was studied (Fig. 7). It has been found that the sorption capacity of PVF sponges increases significantly when moving from unfilled PVF to PVF with AuNPs incorporated *ex situ*, and even more so in relation to PVF with AuNPs incorporated *in situ*.

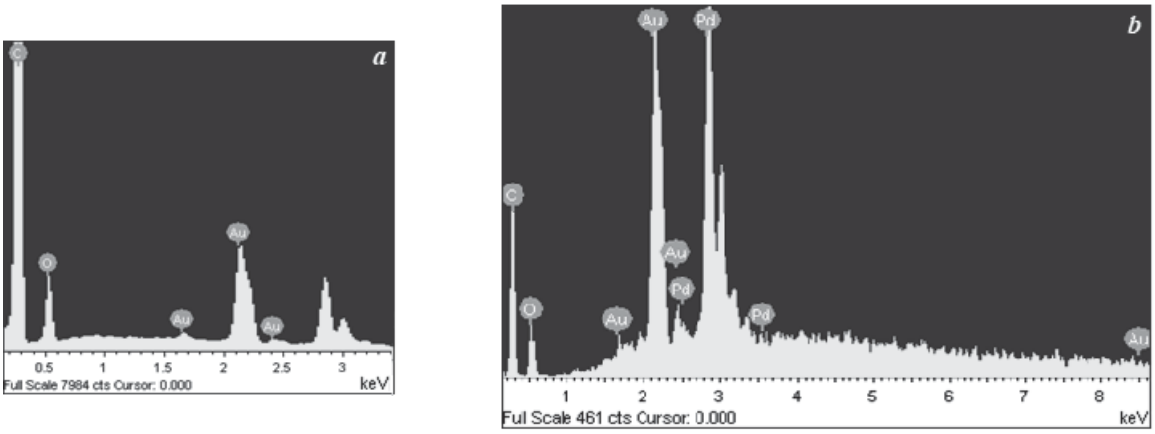

Fig. 6. EDX-spectra of *in situ* (*a*) and *ex situ* (*b*) gels

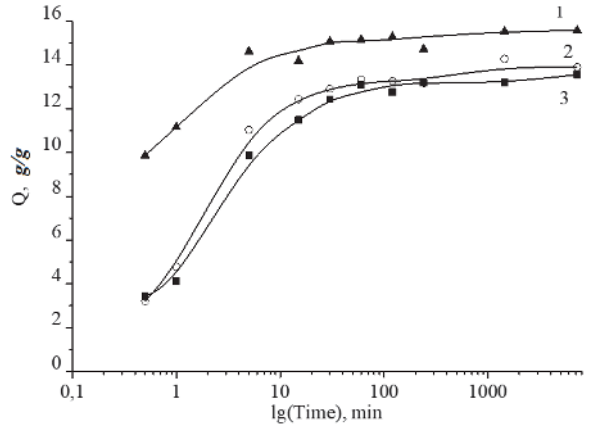

Fig. 7. Swelling kinetics in water of an unfilled PVF sponge (*1*), a PVF sponge with *ex situ* incorporated AuNPs (C = 12 μg/g) (*2*) and a PVF sponge with *in situ* incorporated AuNPs (C = 12 μg/g) (*3*)

Thermal analisys. To evaluate the thermal stability of hybrid hydrogels based on PVF, we conducted TG, DTA, and DTG measurements. Let's analyze their results (Fig. 8, Table 1).

According to the TG data, the mass loss for all the gels studied during the first decomposition stage in the temperature interval from 30 to 200 °C ranged from 5.22 to 7.24 % (in the case of *ex situ* gels). This mass loss is associated with the evaporation of free and weakly bound water, which remains in the gels in small amounts. The main mass loss (about 60 %) in the gels occurs in the temperature range from 200 to 450 °C and is caused by several processes. Complete decomposition of the gels, with a mass loss of about 30%, occurs in the third stage of thermolysis, in the temperature range of 450–575 °C. According to the DTA analysis results for all three hybrid gels, an intensive exothermic peak occurs within the temperature range of 30 to 600–700 °C. It should be noted that complete thermodestruction of *in situ* gels occurs at temperatures approximately 100 °C higher than in the case of *ex situ* gels.

According to the DTG data, all three of the studied gels are characterized by a maximum in

the region of about 80 °C due to the evaporation of unbound water. After reaching a plateau at approximately 115 °C, a smooth thermal release occurs with an additional increase in temperature up to approximately 220-250 °C, likely due to the evaporation of bound water. The most intense peak, around 290–315 °C, likely corresponds to the rupture of the formal ring characteristic to polyvinyl alcohol (PVA), which occurs via a free radical mechanism involving the formation of hydroperoxide under the influence of molecular oxygen. This process leads to the formation of carbonyl groups and the release of formaldehyde [27]. The subsequent peak at approximately 400 °C is likely associated with the dehydration of residual PVA hydroxyl groups (as demonstrated by IR spectroscopy, PVA remains present in the hybrid gel along with PVF) and the formation of a polyene structure. The thermal behavior of hybrid gels in this temperature range is also influenced by their phase transition – melting [28]. This stage of degradation is dominated by chain cleavage, side, and cyclization reactions. OH-group residues act as weak links that provoke chain cleavage of unconjugated polyenes [29]. With an increase in temperature, the thermolysis of preformed polyenes occurs, releasing macro radicals that decompose into low-molecular-weight oxygen-containing products, such as acetaldehyde, acetic acid, benzaldehyde, and acrolein. This process also involves the formation of cis- and trans-derivatives of polyene macro-radicals, as well as products of their intermolecular cyclization, particularly furan. Finally, thermal oxidation occurs in the carbonized residue [30].

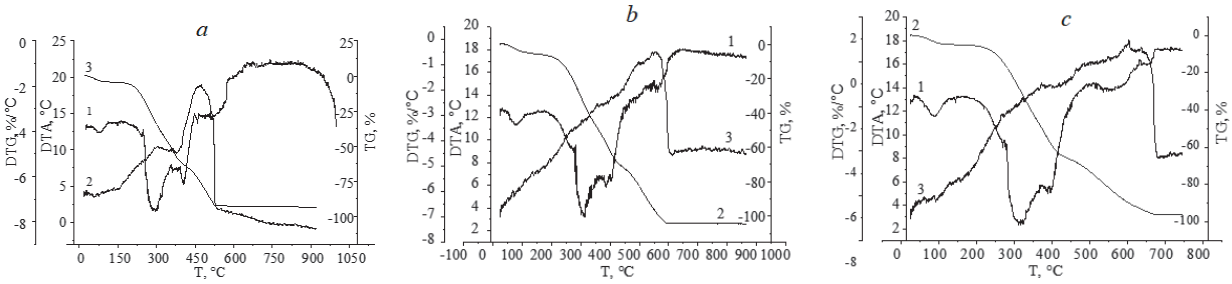

Fig. 8. TG, DTG and DTA curves for PVF sponge: *a – in situ*, *b – ex situ*, *c* – unfilled; *1* – DTG, %/°C, *2* – DTA, °C, *3* –TG, %

Table 1. PVF sponges decomposition stages

Temperature interval, °C	Weight loss, %			
	Unfilled PVF sponge	PVF sponge with AuNPs *in situ*	PVF sponge with AuNPs *ex situ*	Degradation stage
30–200	5.22	5.68	7.24	Free water evaporation
200–450	58.82	59.12	61.47	Bound water evaporation, rupture of the formal ring, melting, water elimination as a result dehydration of residual PVA hydroxyl groups
450–575	29.65	31.04	31.29	Polyenes chain cleavage, side, and cyclization reactions, decomposition into low-molecular-weight oxygen-containing products, ash forming
Total	93.68	95.84	100	

Thus, all synthesized hybrid gels demonstrate thermal stability over a wide temperature range, which significantly exceeds the range of their applications and processing. The results prove that these gels can withstand steam sterilization at 121 °C without significant change. This is important for creating on their base different medical devices and conducting biological and cellular research. The gel obtained by the *in situ* method is more thermally stable than the *ex situ* gel; the *in situ* gel undergoes complete thermal destruction at a temperature 100 °C higher, *i.e.*, 700 °C.

The release of incorporated drugs from hybrid hydrogels is described by saturation curves (Fig. 9). In the case of DOXrubicin intensive, prolonged release of the drug is provided for about 5 hours, followed by a gradual decrease in the diffusion of the anticancer drug. The percentage of Doxorubicin that was washed out was approximately 100 % when gold nanoparticles were incorporated using the *in situ* method, and approximately 90 % when the *ex situ* method was used. The amount of the anticancer drug released during the first five hours was 440 μg for the gel obtained by the *in situ* method, and slightly higher (524 μg) for the hybrid hydrogel synthesised by the *ex situ* method. Unlike Doxorubicin, which has a prolonged sustained release, both hydrogels are characterised by a rapid, almost immediate release of the incorporated Albucid (90 and 87 % for the *in situ* and *ex situ* gels, respectively). Given the mechanism of action of this bacteriostatic agent, it is desirable for its active release to occur at the initial stage, as this leads to the disinfection of the surgical field and prevents secondary infection. On the other hand, the prolonged release of Doxorubicin contributes to its therapeutic function of preventing tumour recurrence.

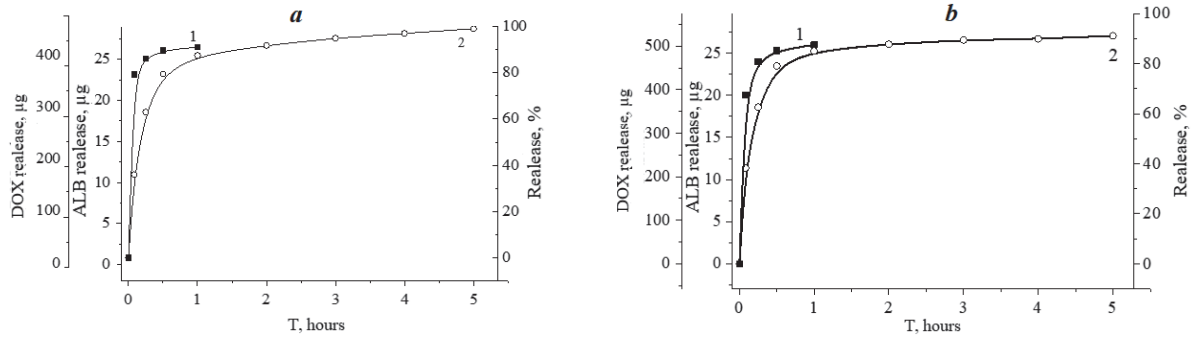

Fig. 9. DOX, ALB release from hybrid hydrogels: (*a*) – *ex situ*, (*b*) – *in situ*

Acute systemic toxicity tests at the molecular level of the obtained hybrid hydrogels were performed based on the parameters related to key enzymatic activities, genotoxicity and cytotoxicity.

Biological membranes are the first barrier that protects the cell from toxic effects of various kinds. One of the most important membrane proteins is adenosine triphosphatase (ATPase), the largest protein complex member of the P-type family of active cation transport proteins [31].

In order to analyse the acute systemic toxicity at the molecular level of the synthesised hydrogels, their effect on the molecular multienzyme complex of cell membranes of the test culture L929 was investigated. This molecular complex exhibits Mg^{2+}-dependent-ATP hydrolase (Mg^{2+}-ATPase) activity, which ensures the generation of transmembrane potential of cells, maintains the physiological level of energy metabolism and energy-dependent metabolic processes in the cell. The key role in ensuring normal cell functioning makes this enzyme complex a highly sensitive biochemical marker of toxicity [32].

The data on the analysis of acute systemic toxicity of samples of hybrid hydrogels based on PVF with gold nanoparticles incorporated both *ex situ* (gold nanoparticles with an average size of 30 nm were incorporated during the synthesis of hydrogels) and *in situ* (the synthesis of AuNPs was carried out directly in the pore space of the hydrogel matrix using a solution of gold chloride hydrochloric acid) are shown in Fig. 10.

Thus, the absence of toxic effects of samples of both the PVF hydrogels with incorporated *ex situ* and *in situ* gold nanoparticles was recorded:

the activity of Mg^{2+}-dependent ATPase activity of cell membranes of the test culture L929 was at the level of this indicator in the negative (native) control.

The study of cytotoxicity of hybrid hydrogels with gold nanoparticles incorporated *ex situ* and *in situ* demonstrated a low level of their cytotoxic effect. Thus, the media conditioned with samples of hybrid hydrogels with gold nanoparticles incorporated both *ex situ* and *in situ* for 24 h had a slight effect on the metabolic activity of L929 cells (about 10 %) in the MTT-test, although the total number of adherent cells decreased by almost 20 % compared to the results of the crystal violet test. The indices of metabolic activation were 0.8–1.1, indicating the non-toxicity of the hybrid hydrogels with gold nanoparticles incorporated *ex situ* and *in situ* media for L929 cells.

Table 2 shows the results of the in vitro genotoxicity analysis of hybrid hydrogels with gold nanoparticles incorporated *ex situ* and *in situ*. As shown in Table 2, the studied hydrogels do not exhibit genotoxic properties.

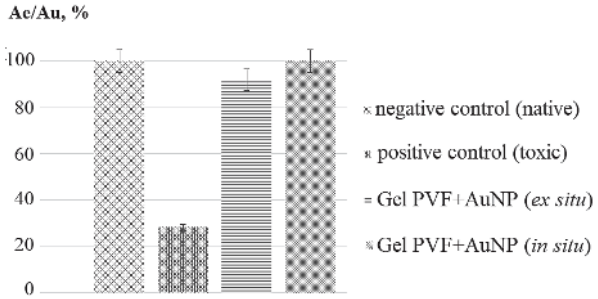

Fig. 10. The level of acute systemic toxicity of PVF samples of hybrid hydrogels with gold nanoparticles incorporated *ex situ* and *in situ* by the nature of the effect on the molecular multienzyme complex (Mg^{2+} – dependent-ATPase activity) of cell membranes of the test culture L929

Table 2. In vitro evaluation genotoxicity of hybrid hydrogels with gold nanoparticles incorporated *ex situ* and *in situ*

Control/Sample	Comet assay index	Conclusion on toxicity
Positive control	2.051±0.001	Genotoxic
Negative control	0.042±0.002	Non genotoxic
Hybrid hydrogels with gold nanoparticles incorporated *ex situ*	0.049±0.001	Non genotoxic
Hybrid hydrogels with gold nanoparticles incorporated *in situ*	0.047±0.002	Non genotoxic

CONCLUSION

Thus, the properties of the synthesized hybrid hydrogels (based on polyvinyl formal and gold nanoparticles incorporated by *ex situ* and *in situ* methods) were characterized using a variety of physicochemical research methods. Both hybrid hydrogels obtained with gold nanoparticles incorporated *ex situ* and *in situ* have been found to have high thermal stability, which significantly exceeds the temperature range of their production, sterilization, and application. The *in situ* hybrid hydrogel is more thermally stable than the *ex situ* gel; the *in situ* gel undergoes complete thermal destruction at a temperature 100°C higher.

According to SEM and EDX results, the concentration of gold nanoparticles was approximately twice as high when incorporated using the *ex situ* method compared to the *in situ* method. However, the latter method produced a much more uniform distribution of gold.

According to the effect on the molecular multienzyme complex of cell membranes of the test culture L929 both obtained hybrid hydrogels with gold nanoparticles incorporated *ex situ* and *in situ* were characterized as nontoxic. Into the cytotoxicity tests the both types of hybrid hydrogels exhibited a low level of toxicity. The absence of genotoxic effect *in vitro* was shown for both studied hydrogel samples. Thus, the hybrid

hydrogels with gold nanoparticles incorporated *ex situ* and *in situ* were characterized as biosafe in the tests of the acute systemic toxicity at the molecular level.

ACKNOWLEDGEMENT

The authors are grateful for the financial support of the National Research Foundation of Ukraine (in the framework of the competition "Science for Security and Sustainable Development of Ukraine) within project "Hybrid hydrogel materials with gold nanoparticles and cytostatics with complex antitumor and regenerative activity for the needs of reconstructive surgery in the oculo-orbital region" (No 2021.01/0178, 2023).

Інкорпорація наночастинок золота методами *in situ* та *ex situ* в гібридні гідрогелі медичного призначення

Д.К. Гончарук, А.П. Малецький, Т.П. Полторацька, Л.О. Керносенко, Н.О. Пасмурцева, М.М. Лазаренко, С.М. Дибкова, Л.С. Резніченко, Т.Г. Грузіна, В.І. Подольська, Ю.М. Самченко

Інститут біоколоїдної хімії ім. Ф.Д. Овчаренка Національної академії наук України
бул. Академіка Вернадського, 42, Київ, 03142, Україна, goncarukdima325@gmail.com
Інститут очних хвороб і тканинної терапії ім. В.П. Філатова Національної академії медичних наук України
Французький бульвар, 49/51, Одеса, Україна, 65061, Україна
Київський національний університет імені Тараса Шевченка
пр-т Академіка Глушкова, 4, Київ, 03680, Україна

Полімерні гідрогелі посідають особливе місце серед матеріалів, що зараз використовуються для виготовлення імплантатів, завдяки своїй структурній подібності до макромолекулярних компонентів, що містяться в організмі людини. Однак традиційні гідрогелі часто мають недостатню механічну міцність, біосумісність та біологічну активність. Щоб подолати ці обмеження, ми розробили методи синтезу композитних гібридних гідрогелів на основі пористого полівінілформалю та наночастинок золота. Було показано, що фізичні та хімічні властивості цих гідрогелів залежать від стратегії синтезу, що використовується для композитного матеріалу, а також від типу та методу синтезу наночастинок, які він містить.

Морфологію синтезованих гібридних гідрогелів (на основі полівінілформалю та наночастинок золота, включених методами in situ та ex situ) досліджували за допомогою електронної мікроскопії (SEM), а їхню хімічну структуру підтверджували за допомогою ІЧ-спектроскопії. Елементний склад синтезованих полімерних нанокомпозитів досліджували за допомогою енергодисперсійної рентгенівської спектроскопії (EDX), а їхню термостабільність та процеси термолізу аналізували за допомогою термогравіметричного аналізу (TG, TGA та DTG дослідження). Було досліджено кінетику набухання гібридних гелів з інкорпорованими наночастинками золота у воді, швидкість дифузії інкорпорованого протипухлинного препарату Доксорубіцину та бактерициду Альбуциду, а також їхній регенеративний ефект та гостру токсичність з використанням клітинних експериментів in vitro.

Синтезовані композитні гібридні гідрогелі на основі пористого полівінілформалю та наночастинок золота є перспективними як імплантатів для реконструктивної хірургії в окулоорбітальній ділянці. Вони також можуть бути використані для заповнення післяопераційних порожнин після резекції пухлини, забезпечуючи стерильність операційного поля та запобігаючи рецидиву пухлини.

***Ключові слова**: гідрогелі, полівінілформаль, губка, імплантати, наночастинки золота, реконструктивна хірургія, орбітальні травми*

REFERENCES

1. Tselomudriy A.I., Venger G.E., Rizvaniuk A.V., Pohoreliy D.N., Putienko V.A. Peculiarities of surgical rehabilitation of soldiers with battle eye wounds in modern conditions. In: *Conference dedicated to the 80th*

anniversary of the Filatov Institute of Eye Diseases and Tissue Therapy of NAMSU and 14th Black Sea Ophthalmological Congress "Filatov Memorial Lectures". 2016. P. 95.
2. Lanigan A., Lindsey B., Maturo S., Brennan J., Laury A. The Joint Facial and Invasive Neck Trauma (J-FAINT). Project, Iraq and Afghanistan: 2011-2016. *Otolaryngology–Head and Neck Surgery*. 2017. **157**(4): 602.
3. Richards J.T., Overmann A., Forsberg J.A., Potter B.K. Complications of Combat Blast Injuries and Wounds. *Current Trauma Reports.* 2018. **4**: 348.
4. Bingham J.R., Bowyer M.W. Combat Soft Tissue Injuries. *Current Trauma Reports*. 2018. **4**: 333.
5. Samchenko Yu.M., Dibkova S.M., Maletsky A.P., Kernosenko L.O., Gruzina T.G., Pasmurceva N.O. Antimicrobial effects of hydrogel implants incorporating gold nanoparticles and albucide and developed for reconstructive surgery in the orbit and periorbital area. *Ophthalmology Journal (Ukraine)*. 2023. **5**: 27.
6. Samchenko Yu.M., Maletsky A.P., Bigun N.M., Dolinsky G.A., Kernosenko L.O., Pasmurceva N.O. Dynamics of deposition and diffusion of drugs (chlorhexidine, 5-fluorouracil, and DOXrubicin) when using hydrogel implants with different densities. *Ophthalmology Journal (Ukraine).* 2020. **3**: 53.
7. Maletskyy A., Maletskyy A., Samchenko Yu., Bigun N. Improving the Antitumor Effect of DOXrubicin in the Treatment of Eyeball and Orbital Tumors. In: *Advances in Precision Medicine Oncology.* Edited by Hilal Arnouk, Bassam Hassan. (London: IntechOpen. 2021).
8. Jafari M., Paknejad Z. Polymeric scaffolds in tissue engineering: a literature review. *J. Biomed. Mater. Res. B Appl. Biomater*. 2017. **105**(2): 431.
9. Ho T.C. Chang C.C., Chan H.P., Chung T.W., Shu C.W., Chuang K.P., Duh T.H., Yang M.H., Tyan Y.C. Hydrogels: properties and applications in biomedicine. *Molecules*. 2022. **27**(9): 2902.
10. Darweesh R.S. Darweesh R.S., Ayoub N.M., Nazzal S. Gold nanoparticles and angiogenesis: molecular mechanisms and biomedical applications. *Int. J. Nanomedicine*. 2019. **14**: 7643.
11. Chugh H., Sood D., Chandra I., Tomar V., Dhawan G., Chandra R. Role of gold and silver nanoparticles in cancer nano-medicine. *Artif. Cells Nanomed. Biotechnol.* 2018. 46(**1**): 1210.
12. Pinho R.A., Haupenthal D.P.S., Fauser P.E., Thirupathi A., Silveira P.C.L. Gold nanoparticle-based therapy for muscle inflammation and oxidative stress. *Int. J. Nanomedicine.* 2022. **15**: 3219.
13. Li H., Pan S., Xia P., Chang Y., Fu C., Kong W., Yu Z., Wang K., Yang X., Qi Zh. Advances in the application of gold nanoparticles in bone tissue engineering. *J. Biol. Eng*. 2020. **14**(1): 14.
14. Yesildag C., Zhang Z., Fang R., G. de Vicente, Lensen M.C. Nano- and micro-patterning of gold nanoparticles on PEG- based hydrogels for controlling cell adhesion. In: *Noble and Precious Metals - Properties, Nanoscale Effects and Applications*. (InTech., 2018).
15. Wu Y., Wang H., Gao F., Xu Z., Dai F., Liu W. An injectable supramolecular polymer nanocomposite hydrogel for prevention of breast cancer recurrence with theranostic and mammoplastic functions. *Adv. Funct. Mater*. 2018. **28**(21): 1801000.
16. Heo D.N., Ko W.K. Enhanced bone regeneration with a gold nanoparticle-hydrogel complex. *J. Mater. Chem. B.* 2014. **2**(11): 1584.
17. Donghyun Lee, Dong Nyoung, Heo Ha Ram Nah, Sang Jin Lee, Wan-Kyu Ko, Jae Seo Lee, Ho-Jin Moon, Jae Beum Bang, Yu-Shik Hwang, Rui L Reis, Il Keun Kwon. Injectable hydrogel composite containing modified gold nanoparticles: implication in bone tissue regeneration. *Int. J. Nanomedicine*. 2018. **13**: 7019.
18. Grant S.A., Zhu J., Gootee J., Snider C.L., Bellrichard M., Grant D.A. Gold nanoparticle-collagen gels for soft tissue augmentation. *Tissue Eng. Part A.* 2018. **24**(13–14): 1091.
19. Tan H.L., Teow S.Y., Pushpamalar J. Application of metal nanoparticle-hydrogel composites in tissue regeneration. *Bioengineering (Basel)*. 2019. **6**(9): 17.
20. Turkevich J., Stevenson P.C., Hillier J. A Study of the Nucleation and Growth Processes in the Synthesis of Colloidal Gold. *Discuss. Faraday Soc.* 1951. **11**: 55.
21. Samchenko Yu., Korotych O., Kernosenko L., Kryklia S., Litsis O., Skoryk M., Poltoratska T., Pasmurtceva N. Stimuli-responsive hybrid porous polymers based on acetals of polyvinyl alcohol and acrylic hydrogels. *Colloids Surf. A*. 2018. **544**: 10443.
22. Safety assessment of medical nanopreparations' approved by the Scientific Expert Council of the State Expert Centre of the Ministry of Health of Ukraine (protocol No 8, 09.26.2013). Guidelines. Kyiv. 2013.
23. Podolska V.I., Rieznichenko L.S., Yakubenko L.M., Gruzina T.G., Zholobak N.M., Samchenko Y.M., Dybkova S.M. A Study on the Interaction of Gold Nanoparticles With Sodium Sulfacetamide. *Him. Fiz. Tehnol. Poverhni.* 2024. **15**(3): 349. [in Ukrainian].
24. Poly(vinyl formal) (9003-33-2) IR Spectrum. In: *ChemicalBook*, accessed July 21, 2024. [e-resource].
25. Nakamoto K. Infrared and Raman Spectra of Inorganic and Coordination Compounds. In: *Part A. Theory and Applications in Inorganic Chemistry*. (NJ: John Wiley & Sons, Inc., 2008).
26. Silverstein R.M., Webster F.X., Kiemle D.J. *Spectrometric Identification of Organic Compounds.* 7th ed. (NJ: John Wiley & Sons, 2005).

27. Chanda M., Kumar W.S.J., Raghavendrachar P. A Kinetic Investigation of the Thermal Degradation of Poly(Vinyl Formals). *J. Appl. Polym. Sci.* 1979. **23**(3): 755.
28. Guirguis O., Moselhey M. Thermal and structural studies of poly (vinyl alcohol) and hydroxypropyl cellulose blends. *Nat. Sci*. 2012. **4**: 57.
29. Morancho J.M., Salla J.M., Cadenato A., Fernández-Francos X., Ramis X., Colomer P., Ruíz R. Kinetic Studies of the Degradation of Poly(Vinyl Alcohol)-Based Proton-Conducting Membranes at Low Temperatures. *Thermochimica Acta*. 2011. **521**(1–2): 139.
30. Budrugeac P. Kinetics of the Complex Process of Thermo-Oxidative Degradation of Poly(Vinyl Alcohol). *J. Therm. Anal. Calorim.* 2008. **92**(1): 291.
31. Radosinska D., Kovalcikova G., Gardlik A., Chomova R., Snurikova M., Radosinska D., Vrbjar N. Oxidative Stress Markers and Na,K-ATPase Enzyme Kinetics Are Altered in the Cerebellum of Zucker Diabetic Fatty fa/fa Rats: A Comparison with Lean fa/+ and Wistar Rats. *Biology*. 2024. **13**(10): 759.
32. Vasić V., Momić T., Petković M., Krstić D. Na^+, K^+-ATPase as the target enzyme for organic and inorganic compounds. *Sensors (Basel)*. 2008. **8**(12): 8321.

Received 11.07.2025, accepted 04.12.2025